ISSN 1330-3651 (Print), ISSN 1848-6339 (Online) https://doi.org/10.17559/TV-20220727092344
Original scientific paper

Modelling Grounding Systems Using the Finite Element Method: The Influence of the Computational Domain Size on the Accuracy of the Numerical Calculation

Tomislav BARIĆ, Hrvoje GLAVAŠ, Željko HEDERIĆ, Mirko KARAKAŠIĆ*

Abstract: Simulating the static and dynamic behaviour of grounding systems using numerical methods is a well-established procedure. In order to achieve greater model accuracy, a special attention is usually paid to the construction of more complex models. However, in the modelling process, there are certain factors that have a great influence on the model accuracy regardless of its complexity. They can drastically reduce the accuracy of high-quality complex models. The article elaborates on the ratio influence of the soil dimensions and the dimensions of the buried part of the grounding system, i.e. the influence of the edge distance of the hemispherical soil model from the centre of the grounding system (i.e. computational domain size) on the accuracy of the numerical calculation using the finite element method. In this paper, the physical cause of the influence of the computational domain size on the accuracy of the calculation is explained in detail. The paper gives a mathematical model that accurately describes the influence of the edge distance of the hemispherical soil model from the grounding conductors on the accuracy of the numerical calculation. Based on the presented theory, derived expressions and simulation results, guidelines in the implementation of numerical methods in modelling grounding systems are given. Also, the applicability of these guidelines in other applications such as modelling, analysis and interpretation of resistance data using FEM was considered.

Keywords: accuracy; boundary conditions; computational domain size; finite element method (FEM); grounding system; modelling

1 INTRODUCTION

Due to their exceptional importance in technical applications, grounding systems [1-13] have been extensively analysed in the past. With the development of numerical methods [14, 15], such as the finite element method (FEM) [16], and the boundary element method (BEM), also known as the method of moments (MoM) [17], analyses are performed almost exclusively by computer simulations. Other numerical procedures are also used but to a much lesser extent. Numerical methods in electromagnetism are a very developed branch of electrical engineering and enable obtaining highly accurate results in simulations. However, during the modelling process itself, it is necessary to pay attention to certain factors that affect the results accuracy. The paper describes the influence of the computational domain size, i.e. the edge distance of the hemispherical soil model from the centre of the grounding system on the accuracy of determining grounding resistance and distribution of electric potential on the soil surface. Namely, it is a well-known fact that FEM is not suitable for the solution of the electromagnetic problems with an infinite and a semi-infinite domain (i.e. soil in determining the grounding resistance). BEM is suitable for these tasks. For this reason, commercial software packages for calculating grounding resistance and electrical potential near a grounding system are based on BEM. In short, FEM can directly deal only with bounded computational domains (soil in this type of a problem). This inherent disadvantage of FEM compared to BEM can be overcome if the computational domain is artificially bounded. In the analysed example, the naturally infinite computational domain (the half-space in which the grounding conductor is buried) is modelled with finite dimensions, i.e. with hemisphere. But due to the difficult treatment of inhomogeneous and nonlinear electromagnetic problems using BEM, which is not the case with FEM, the use of FEM in electromagnetic problems with infinite and semi-infinite domains is very common. Scientific curiosity has led us to investigate, in a relatively simple case of a grounding system, the impact of a computational domain size on an error in such an approach. By choosing a relatively simple grounding system, for which there are accurate mathematical models, this paper has shown that it is possible to skilfully use the models to physically explain why the naturally infinite computational domain (the half-space in which the grounding conductor is buried) with the finite computational domain size (i.e. with a hemisphere) causes an error in the calculation. Although the presented expressions are not a scientific novelty, the way they were used with the aim of explaining and estimating the FEM error are, as far as the authors know, the novelty thus scientifically contributing to the research community. Although there may be doubts whether the conclusions drawn from such simple examples of grounding systems can be applied to more complex grounding systems, the validity of the presented approach can be justified as follows. From the quasi-static field theory, it is known that, in the far field region, field acts as if it was caused by a spherical field source or a point field source. Therefore, for distant points in space (far from the grounding system of an arbitrary shape), the current field and electric potential in the soil act as if they were caused by a spherical grounding conductor. Since the transition from the near field to the far field is gradual and depends on the complexity of the grounding system, the data obtained in the previously described way can only serve as indicative values of the actual error in the case of complex grounding systems and they are useful in formulating guidelines. Due to the aforementioned, the guidelines for the initial design phase and analysis of the grounding system using FEM are given separately from the guidelines for more accurate calculations using FEM. Nevertheless, in order to verify the validity of the previously stated approach, the previously presented approach was tested on the example of a complex grounding system. Using a mathematical model, we have shown that modelling naturally infinite computational domain (the half-space where the grounding conductor is buried) with the finite computational domain size (i.e. a hemisphere where the grounding conductor is buried) corresponds to the spatial shift of the boundary condition. Consequently, the boundary conditions of zero potential are no longer infinitely far from the grounding system but rather at a finite distance. Therefore, the influence of boundary conditions that naturally belong to an infinitely distant point begins to be reflected in the accuracy of the numerical calculation. In this paper, the soil is modelled as a homogeneous medium. Also, the soil is modelled as a hemisphere whose radius is larger than the equivalent dimension of the buried part of the grounding system. The grounding system is a vertically buried pipe of a circular cross-section. The grounding system is excited by a current source. By conducting successive simulations at different soil dimensions with unchanged dimensions of the grounding conductor, these dimensions ratio influence on the accuracy of the simulation results was analysed. Based on the presented theory, derived expressions and simulation results, guidelines in the implementation of numerical methods in modelling grounding systems using FEM are given. Also, the applicability of these guidelines in other applications such as modelling, analysis and interpretation of resistance data using FEM was considered.

The rest of this paper is organized as follows. Section 2 explains a grounding system model by which the influence of soil dimensions on the accuracy of the calculation of the grounding resistance and scalar potential can be explained. In section 3, an analytical approach in modelling of a vertically buried cylindrical conductor is presented. Section 4 describes the modelling of a vertically buried cylindrical conductor using FEM. Also, the results of a numerical calculation based on FEM are presented. Section 5 describes the modelling of a complex grounding system using FEM. Also, the results of a numerical calculation based on FEM are presented. The results obtained by analytical methods and FEM are discussed in Section 6. The applicability of the guidelines presented in this paper, such as the analysis and interpretation of resistance data, is presented in Section 7. Finally, conclusions and guidelines are made in the last section.

2 MATHEMATICAL MODEL

The influence of soil dimensions (computational domain size), i.e. the distance of boundary conditions from the centre of the grounding system on the accuracy of the numerical calculation can be analysed by different models. This section elaborates on the grounding system model used to explain the influence of soil dimensions on the calculation accuracy of the grounding resistance and scalar potential. In order to use the simplest possible mathematical model, without losing generality, a buried conductive hemisphere was chosen for the grounding conductor, Fig. 1 and Fig. 2. The grounding system shown in Fig. 1 and Fig. 2 consists of a buried conductive hemisphere of radius R_a and an above ground conductor. The above ground conductor is shown for consistency but is neither relevant for determining the grounding resistance, nor for a potential distribution at the soil surface. The hemispherical conductor is buried in the ground and its upper surface lies in the soil-air plane.

The soil was modelled as a homogeneous medium with constant electrical resistivity. In order to achieve a symmetry of boundary conditions and finite soil dimensions, the soil was modelled as a hemisphere of radius.

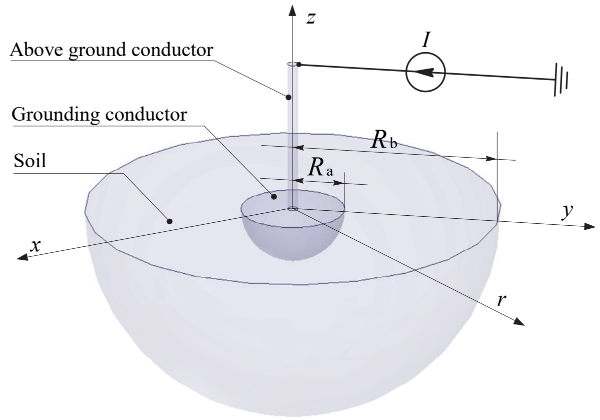

Figure 1 3D graphic representation of the ground (soil), hemispherical grounding conductor and current excitation

The centre of the hemisphere by which the soil is modelled is also the centre of the hemisphere by which the grounding conductor is modelled.

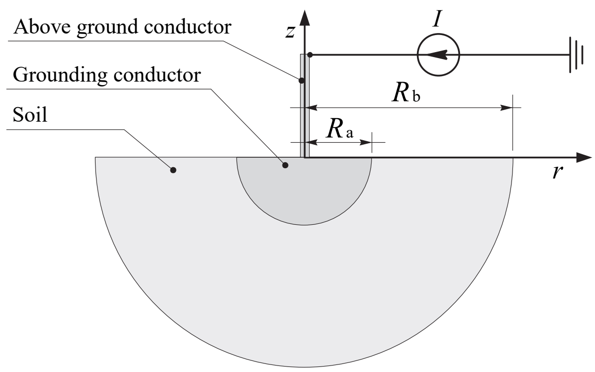

Figure 2 2D graphic representation of the ground (soil), hemispherical grounding conductor and current excitation

The vector field of the current density in soil is determined by the expression [15]:

$$\vec{J} = \frac{I}{S}\vec{a}_{\mathrm{r}} \tag{1}$$

where I is the current injected into a hemispherical grounding conductor, $\vec{a}_{\mathrm{r}}$ is a unit vector perpendicular to the surface of the hemisphere, S is the surface of a hemisphere whose radius is r measured from the centre of the hemispherical conductor.

$$S = 2r^2\pi \tag{2}$$

The relationship between the current density and electric field is determined by relation [15]:

$$\vec{J} = \sigma\vec{E} \tag{3}$$

where σ is electrical conductivity of the soil, and is related to electrical resistivity ρ of the soil by expression [15]:

$$\sigma = \frac{1}{\rho} \tag{4}$$

Combining the previous four expressions gives:

$$\vec{E} = \frac{I\rho}{2\pi}\frac{1}{r^2}\vec{a}_{\mathrm{r}}\,. \tag{5}$$

In quasi-static conditions, the relationship between the electric potential and electric field is described by expression [15]:

$$\vec{E} = -\mathrm{grad}\varphi \tag{6}$$

By integrating the previous expression along the path bounded by points "a" and "b", the expression for the potential difference (voltage) between points "a" and "b" is obtained:

$$U_{\mathrm{ba}} = \varphi_{\mathrm{b}} - \varphi_{\mathrm{a}} = -\int_{\mathrm{a}}^{\mathrm{b}} \vec{E}\cdot \mathrm{d}\vec{s} \tag{7}$$

where the differential element of the path is given by the expression:

$$\mathrm{d}\vec{s} = \vec{a}_{\mathrm{r}} \cdot \mathrm{d}r \tag{8}$$

Inserting expressions (5) and (8) into (7) gives:

$$U_{\mathrm{ba}} = -\int_{r=R_{\mathrm{a}}}^{r=R_{\mathrm{b}}} \left(\frac{I\rho}{2\pi}\frac{1}{r^2}\vec{a}_{\mathrm{r}}\right)\cdot \vec{a}_{\mathrm{r}}\cdot \mathrm{d}r \tag{9}$$

Taking into account $U_{\mathrm{ba}} = -U_{\mathrm{ab}}$, after minor editing of the previous expression, gives:

$$U_{\mathrm{ab}} = \left(\frac{I\rho}{2\pi}\right)\int_{r=R_{\mathrm{a}}}^{r=R_{\mathrm{b}}} \frac{1}{r^2}\left(\vec{a}_{\mathrm{r}}\cdot\vec{a}_{\mathrm{r}}\right)\mathrm{d}r \tag{10}$$

Since $\vec{a}_{\mathrm{r}}\cdot\vec{a}_{\mathrm{r}} = 1$, the previous expression is simplified to:

$$U_{\mathrm{ab}} = \left(\frac{I\rho}{2\pi}\right)\int_{r=R_{\mathrm{a}}}^{r=R_{\mathrm{b}}} \frac{\mathrm{d}r}{r^2} \tag{11}$$

The integration of the previous expression gives:

$$U_{\mathrm{ab}} = \left(\frac{I\rho}{2\pi}\right)\left[-\frac{1}{r}\right]_{r=R_{\mathrm{a}}}^{r=R_{\mathrm{b}}} = \left(\frac{I\rho}{2\pi}\right)\left(-\frac{1}{R_{\mathrm{b}}}+\frac{1}{R_{\mathrm{a}}}\right) \tag{12}$$

A minor rearrangement of the previous expression gives:

$$U_{\mathrm{ab}} = \left(\frac{I\rho}{2\pi}\right)\left(\frac{1}{R_{\mathrm{a}}}-\frac{1}{R_{\mathrm{b}}}\right) \tag{13}$$

Or, in a slightly different form:

$$U_{\mathrm{ab}} = \frac{I\rho}{2\pi}\frac{R_{\mathrm{b}}-R_{\mathrm{a}}}{R_{\mathrm{a}}R_{\mathrm{b}}} \tag{14}$$

The resistance of the soil layers between points "a" and "b" is determined by the expression:

$$R_{\mathrm{ab}} = \frac{U_{\mathrm{ab}}}{I} \tag{15}$$

A substitution of the expression (14) into the expression (15) gives:

$$R_{\mathrm{ab}} = \frac{\rho}{2\pi}\frac{R_{\mathrm{b}}-R_{\mathrm{a}}}{R_{\mathrm{a}}R_{\mathrm{b}}} \tag{16}$$

Expression (16) makes it possible to determine the grounding resistance when the grounding conductor is buried in infinite soil.

$$R_{\infty} = \lim_{R_{\mathrm{b}}\to\infty}\frac{\rho}{2\pi}\frac{R_{\mathrm{b}}-R_{\mathrm{a}}}{R_{\mathrm{a}}R_{\mathrm{b}}} = \frac{\rho}{2\pi}\lim_{R_{\mathrm{b}}\to\infty}\frac{R_{\mathrm{b}}-R_{\mathrm{a}}}{R_{\mathrm{a}}R_{\mathrm{b}}} \tag{17}$$

Further procedure is shown as follows:

$$R_{\infty} = \lim_{R_{\mathrm{b}}\to\infty}\frac{\rho}{2\pi}\frac{1-\frac{R_{\mathrm{a}}}{R_{\mathrm{b}}}}{R_{\mathrm{a}}} \lim_{R_{\mathrm{b}}\to\infty}\frac{\rho}{2\pi}\frac{1}{R_{\mathrm{a}}}\left(1-\frac{R_{\mathrm{a}}}{R_{\mathrm{b}}}\right) = \frac{\rho}{2\pi}\frac{1}{R_{\mathrm{a}}} \tag{18}$$

By introducing the factor:

$$K = K(R_{\mathrm{a}}, R_{\mathrm{b}}) = 1-\frac{R_{\mathrm{a}}}{R_{\mathrm{b}}} \tag{19}$$

It is possible to establish a functional relationship between the grounding resistance in infinite soil and grounding resistance when the conductor is buried in soil modelled with finite dimensions:

$$R = R_{\infty}K \tag{20}$$

The effect of introducing an error into the determination of the grounding resistance due to soil modelling, which is by nature of infinite dimensions with finite dimensions, can be analysed through the error of determining the grounding resistance. The error is defined by the expression:

$$p_{\%} = \frac{R-R_{\infty}}{R_{\infty}}\cdot 100\% = (K-1)\cdot 100\% \tag{21}$$

Substituting (19) into the previous expression results in

$$p_{\%} = -\frac{R_{\mathrm{a}}}{R_{\mathrm{b}}}\cdot 100\ \% \tag{22}$$

The errors of determining the grounding resistance for different ratios $R_{\mathrm{a}}/R_{\mathrm{b}}$ are summarised in Tab. 1.

Table 1 Dependence of the error on the ratio R_a/R_b

Ratio R_b/R_a	2	5	10	20	50
Ratio R_a/R_b	0,5	0,2	0,1	0,05	0,02
K	0,5	0,8	0,9	0,95	0,98
Error p%	−50	−20	−10	−5	−2

2.1 Distribution of Electric Potential at Soil Surface

The influence of boundary conditions, i.e. the distance of boundary conditions from the centre of the grounding system on the distribution of electric potential at the soil surface can be analysed in a similar way.

From Eq. (6) it follows:

$$\varphi = -\int \vec{E} \cdot \mathrm{d}\vec{s} \tag{23}$$

The substitution of (7) and (8) in the previous expression gives:

$$\varphi = -\frac{I\rho}{2\pi}\int \frac{\mathrm{d}r}{r^2} \tag{24}$$

The integration of the previous expression gives [18]:

$$\varphi = \frac{I\rho}{2\pi}\frac{1}{r} + C \tag{25}$$

where C is an unknown integration constant, and is determined from the boundary condition.

By setting the boundary condition according to which the reference zero potential is located at points that are at a distance of from the centre of the grounding system, i.e.

$$\varphi_b = \varphi(R_b) = 0 \tag{26}$$

Then from (25) it follows:

$$C = -\frac{I\rho}{2\pi}\frac{1}{R_b} \tag{27}$$

Combining expressions (25) and (27) gives an expression for the scalar electric potential in the space around the hemispherical grounding conductor when the ground is modelled with finite dimensions:

$$\varphi = \varphi(r) = \frac{I\rho}{2\pi}\left(\frac{1}{r} - \frac{1}{R_b}\right) \tag{28}$$

Using the previous expression, the potential of the grounding conductor can be determined when the ground is modelled with finite dimensions [18]:

$$\varphi_a = \varphi(r = R_a) = \frac{I\rho}{2\pi}\left(\frac{1}{R_a} - \frac{1}{R_b}\right) \tag{29}$$

When the ground is modelled as an infinite medium, more precisely an infinite half-space in which the grounding conductor is buried, then the reference point of the zero potential is in infinity, i.e. the boundary condition is:

$$\varphi_b = \varphi(r \to \infty) = 0 \tag{30}$$

Then from (25) it follows:

$$C = 0 \tag{31}$$

The scalar potential on the soil surface in the case of soil of finite dimensions (dashed curve) and in the case of soil of infinite dimensions (full curve) is shown in Fig. 3.

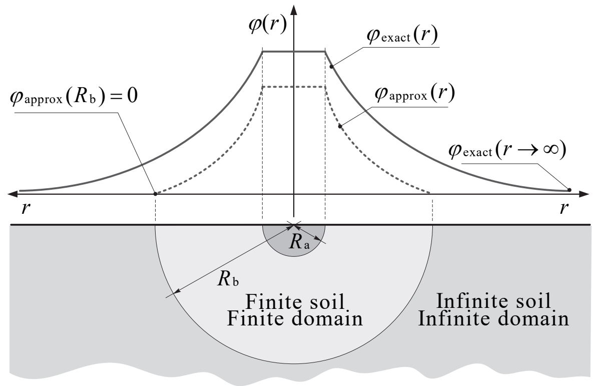

Figure 3 Scalar potential on soil surfaces near the hemispherical grounding conductor

Both potential curves have a constant part for $-R_a \le r \le R_a$, which results from the quasi-static approach of solving the electromagnetic problem, according to which all points along the conductor are at the same potential. For $r > R_a$, both scalar potential curves are monotonically decreasing functions. When the zero potential reference point is at infinity, the scalar electric potential curve at the ground surface has a higher initial value compared to the scalar electric potential curve at the ground surface when the zero potential reference point is set to the distance R_b. The potential gradient ($\mathrm{d}\varphi / \mathrm{d}x$) is the same for both potential curves. This is to be expected since the functions used to describe the potentials in both cases, Eq. (25) differ only by the integration constant C and the derivation of the constant is equal to zero. The correct potential curve is the one that refers to the case when the zero potential reference point is set to infinity. Therefore, when calculating the errors resulting from the use of the potential curve, its values are considered accurate. Assuming that the ground is of finite dimensions, that is, placing a point of the reference zero potential at the distance R_b, makes an error in determining: touch voltage, step voltage and grounding resistance.

3 MODELLING A VERTICALLY BURIED CYLINDRICAL CONDUCTOR: ANALYTICAL APPROACH

In order to make the physical picture as clear as possible and the mathematical model as simple as possible, the hemispherical grounding conductor was chosen in the previous section. However, the hemispherical grounding conductor has little practical significance. For this reason, a relatively simple but widespread grounding system needs to be selected for a further analysis. It should be simple because such grounding systems are very accurate analytical expressions for determining physical quantities such as the grounding resistance and scalar electric potential on the ground surface. This is important because it allows the evaluation of the results of numerical calculations using the finite element method (FEM). A grounding system, which is simple in geometry and very commonly used, consists of vertically buried cylindrical conductors. This paper focused on a system that has only one buried cylindrical conductor (Fig. 4 and Fig. 5).

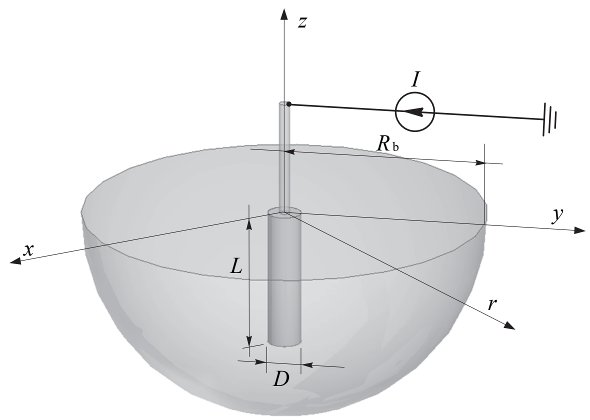

Figure 4 3D graphic representation of the ground (soil), vertical cylindrical conductor and current excitation

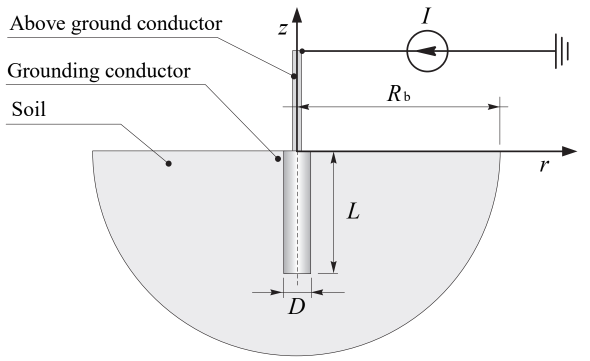

Figure 5 2D graphic representation of the ground (soil), vertical cylindrical conductor and current excitation

The grounding system shown in Fig. 4 consists of a buried conductive cylindrical rod of diameter D and length L and the above ground conductor. The above ground conductor is shown for consistency but is neither relevant for determining the grounding resistance, nor for a potential distribution at the soil surface. The cylindrical conductor is buried in the ground, and its upper surface lies in the soil-air plane. In this case, since the length of the grounding conductor is significantly greater than the diameter, the equivalent dimension of the grounding system is the length of the grounding conductor. The soil was modelled as a homogeneous medium with the constant electrical resistivity. In order to achieve a symmetry of boundary conditions and finite soil dimensions, the soil was modelled as a hemisphere of radius R_b. The centre of the hemisphere by which the soil is modelled is also the centre of the cylindrical grounding conductor.

For this type of the grounding system, there are analytical expressions that can be used to determine the exact scalar electric potential on the ground surface, the potential of the grounding conductor and the grounding resistance. The expressions for the scalar electric potential in the space around a vertical cylindrical grounding conductor are well known in the literature and were obtained using the method of images [15, 19]. According to the method of images, the current field and scalar potential in the soil ($z \geq 0, r \geq D/2$) can be determined in such a way that the domain (the soil in which the grounding conductor is buried (Fig. 6a) is extended by the addition of its mirror image with respect to a symmetry plane, i.e. the boundary between air and soil. In this context, the grounding conductor formally has a double length (the original length plus the length of the mirrored conductor), and is surrounded by a medium that has the same conductivity as soil (Fig. 6b).

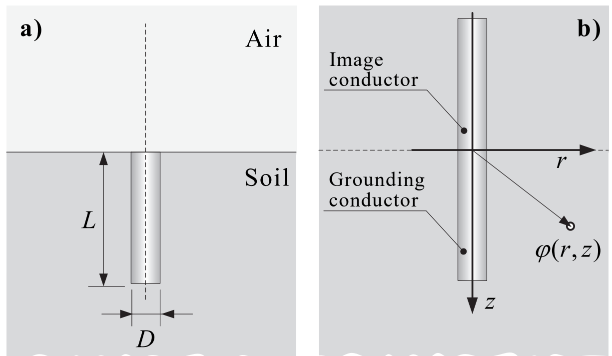

Figure 6 a) Buried vertical cylindrical grounding rod and b) Model for determining scalar electric potential using the method of image

Given the detailed derivation of the expressions in the previous section, which provided a clear idea of how to obtain expressions for the scalar potential and grounding resistance, and since the same procedure applies to the vertical cylindrical grounding rod, the review of analytical expressions will be more concise in this section. The scalar electric potential in the space ($z \geq 0, r \geq D/2$) around the vertical cylindrical grounding conductor is given by the expression [3, 15, 19]:

$$\varphi(z,r) = \frac{I\rho}{4\pi L}\ln\frac{z+L+\sqrt{(z+L)^2+r^2}}{z-L+\sqrt{(z-L)^2+r^2}}+C \quad (32)$$

where I is the current injected into the cylindrical grounding conductor (A), ρ is the electrical resistivity of the soil (Ωm), L is the length of the buried part of the grounding conductor (m), C is an unknown integration constant, which is determined from the boundary condition. Its meaning in the Eq. (32) is identical to the meaning in the Eq. (25), and is determined in the same way.

When the soil is of the infinite size, the zero potential reference point is set at an infinite distance from the grounding system $\varphi\ (z=0, r\to\infty)=0$, then the constant C is:

$$C = 0 \quad (33)$$

When the soil is finite in size, the zero potential reference point is set at the finite distance from the grounding system $\varphi\ (z=0, r=R_b)=0$, then the constant C is:

$$C = -\frac{I\rho}{4\pi L}\ln\frac{L+\sqrt{L^2+R_b^2}}{-L+\sqrt{L^2+R_b^2}} \tag{34}$$

Using Eq. (32) to Eq. (34), we can obtain curves of the approximate and exact dependence of the scalar electric potential on the soil surface (z = 0). The approximate and exact dependence of the scalar electric potential on the ground surface near the vertical cylindrical grounding conductor is shown in Fig. 7.

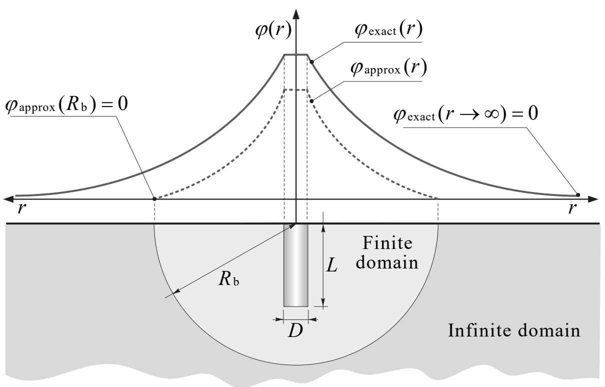

Figure 7 Scalar potential on soil surfaces in the vicinity of the cylindrical grounding conductor

Given the relatively simple geometry, the grounding resistance of a vertical rod buried in the ground can be calculated with high accuracy using analytical expressions. One such very common expression is [20, 24, 25]:

$$R = \frac{\rho}{2\pi L}\left(\ln\frac{8L}{D}-1\right) \tag{35}$$

For the numeric values $\rho = 100\ \Omega\text{m}$, L = 2 m, D = 5 cm, according to the previous expression is obtained $R = 37{,}96\ \Omega$. The obtained value will serve as a control value as to whether the numerical calculation using the finite element method is well performed. Should a significant deviation occur, this would indicate that the simulation settings using FEM are incorrect.

4 MODELLING A VERTICALLY BURIED CYLINDRICAL CONDUCTOR: FEM APPROACH

In general, electromagnetic problems, as presented, can be described by an integral or differential equations. If they are described by integral equations, then the system of integral equations is solved by applying the Boundary element method. Such an approach in the grounding system simulation and the analysis uses a well-known CDEGS [21] software package. If the electromagnetic problem is described by differential equations, then the finite element method is typically used to solve them. Well-known software packages that use that approach are Ansys [22] and Comsol [5, 23]. In this paper, the numerical calculation is performed using the finite element method. For this purpose, the software package Ansys-Maxwell [22] was used. Modelling a grounding system using modern FEM based software packages is very fast and simple with a similar procedure that must be performed in the modelling process. To illustrate the above, several important steps have been selected and shown. The modelling process of the grounding system begins by drawing the appropriate geometries of the grounding system (represented by a vertical cylinder) and soil (represented by a hemisphere). This is followed by the association of the appropriate material with the specified geometries, i.e. the electrical properties of the materials. After that, it is necessary to choose the excitation type. In this article, the current excitation is selected. The current of one ampere was injected into the upper base of the grounding conductor (Fig. 8a). This was achieved by choosing a current excitation called "current source". The curved surface of the hemisphere is associated with a current excitation called "current sink" (Fig. 8b).

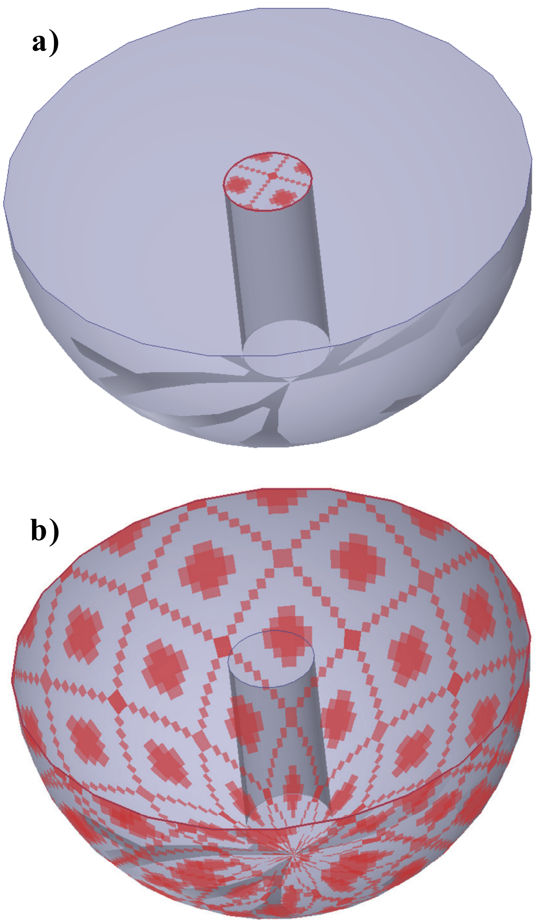

Figure 8 Current excitation a) With current source (current injection) along the upper base of the grounding conductor; b) With current sink along the curved part of the hemisphere by which the soil is modelled

This means that, at the model level, all injected current in the grounding conductor is extracted through the curved half of the hemisphere by which the soil is modelled.

This is followed by segmentation (Fig. 9a), i.e. the division of the computational domain into a finite number of elements. The segmentation of the computational domain was done by limiting the number of elements to 10000 elements (for the lowest R_B / L ratio). Then, as the computational domain increased (higher R_B / L ratio), the limit of the number of finite elements was increased in proportion to the size of the computational domain. Next, we selected an adaptive solver setup with a maximum number of pass equal to 20 and a percentage error of 0,1%.

We used DC conduction solver. In DC conduction solver the FEM computational formulation is based on Eq. (3) and Eq. (6). In DC conduction solver, the quantity solved is the electric scalar potential. Current density and electric field are automatically calculated from the electric scalar potential. The grounding resistance is determined as follows. On the soil surface, from the centre of the grounding conductor to the boundary of the computational domain, a polyline is drawn (Fig. 9b).

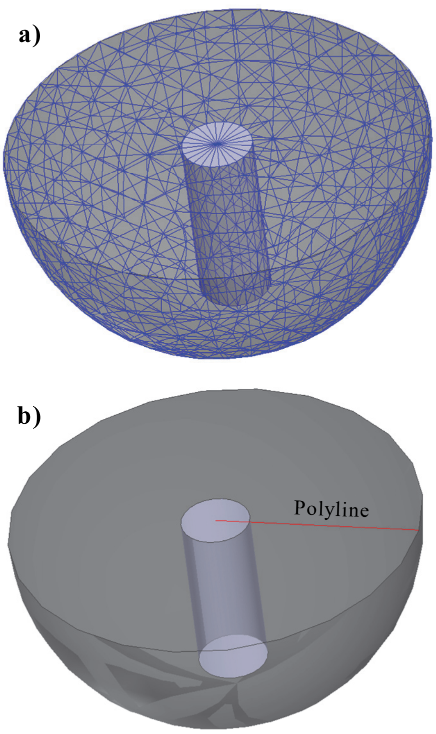

Figure 9 a) Computational domain segmentation; b) Polyline position within the model

The calculated potential along the polyline can be accessed by making a Field Report.

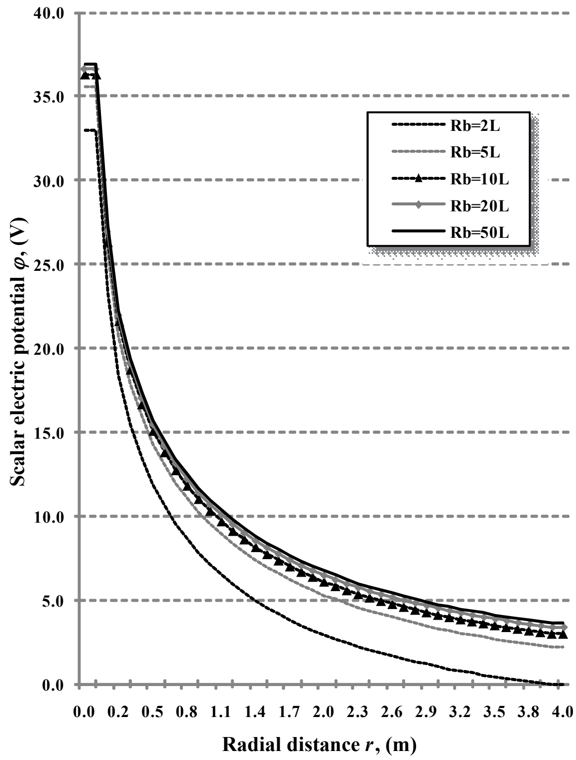

Figure 10 Scalar electric potential on the ground surface (z = 0) as a function of the radial distance

Using this technique, Fig. 10 was obtained. Potential values for radial distances that are smaller than the grounding conductor radius correspond to the grounding system potential. Then, according to Eq. (15), where "I" is the injected current into the grounding conductor, the grounding resistance is determined. Using the previously described model, a numerical calculation was performed. The numerical calculation included the determination of the scalar electric potential (Fig. 10) on the soil surface and the grounding resistance (Tab. 2). Multiple calculations were performed for different parameter i.e. ratio R_B / L .

Table 2 Grounding resistance obtained by using FEM

Ratio R_b/L	2	5	10	20	50	100
Grounding resistance R / Ω	32,99	35,56	36,30	36,62	36,96	37,17
Change compared to the previous calculation	0	2,57	0,74	0,32	0,34	0,21
Relative change compared to the previous calculation / %	0	7,79	2,08	0,88	0,93	0,56
Error in relation to the analytical expression / %	−13,09	−6,32	−4,37	−3,53	−2,63	−2,08

The soil was modelled as a homogeneous medium with the constant electrical resistivity $\rho = 100\ \Omega\text{m}$. In order to achieve the symmetry of the boundary conditions and finite soil dimensions, the soil was modelled as a hemisphere of radius R_b. The centre of the hemisphere by which the soil is modelled is also the centre of the cylindrical rod by which the grounding conductor is modelled. The length of the cylindrical rod is L = 2 m, and the diameter is D = 5 cm. The current injected into the grounding conductor is I = 1 A.

5 MODELLING A COMPLEX GROUNDING SYSTEM: FEM APPROACH

In this section, a complex grounding system is modelled and analysed. That is, the impact of a computational domain size on an error in the calculation of grounding resistance using FEM in the case of a complex grounding system. An equally spaced grounding grid was selected for the complex grounding system (Fig. 11a). This type of grounding system is typically used for substation grounding. Due to its importance for safety in AC substation, this type of grounding is described in detail in IEEE Std 80-2000 [24]. Specified standard provides grounding resistance for certain dimensions of grounding grids. For this reason, we chose a grounding grid for which grounding resistance is given in [24]. We chose four mesh grounding grid with sides measuring 30 m × 30 m. The grounding grid is at 1 m depth, and the soil resistivity is 100 Ωm. According to [24], the grounding resistance of such a grounding system is exactly 1,7 Ω (Fig. 11b taken and processed from [24]). We will consider this value of grounding resistance to be exact and in relation to this value we will determine the error of numerical calculation using FEM for different ratio $R_b/D_{eqv.}$.

Using the previously described model, a numerical calculation of the determination of grounding resistance was performed. Multiple calculations were performed for different ratio $R_b/D_{eqv.}$. The results of the numerical calculation are summarized in Tab. 3. Also, for the ratio $R_b/D_{eqv.} = 2$, scalar electric potential on the ground surface and scalar electric potential along the cross section of the computational domain are shown (Fig. 12).

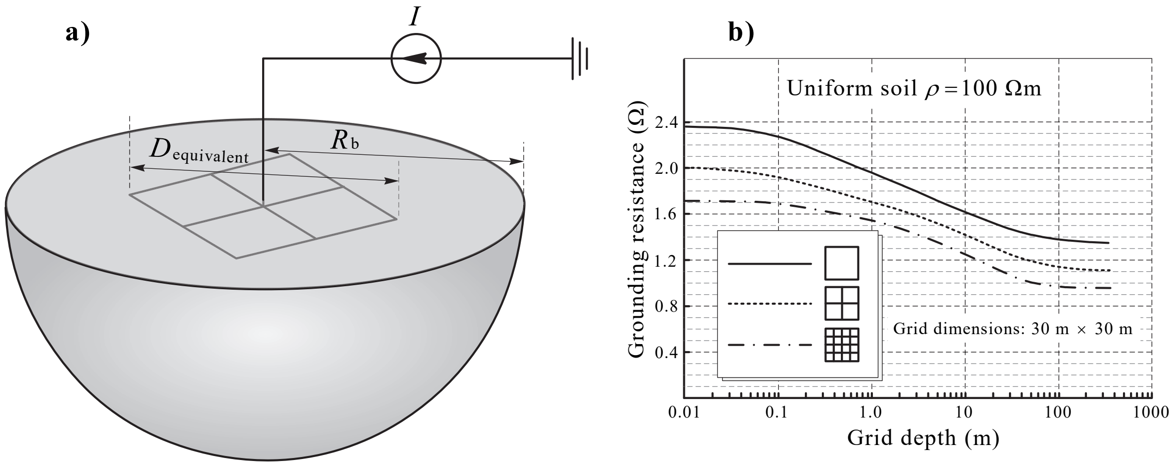

Figure 11 a) 3D graphic representation of the ground (soil), four mesh grounding grid and current excitation; b) Grid resistance versus grid depth

Table 3 Grounding resistance obtained by using FEM

Ratio $R_b/D_{eqv.}$	2	5	10	20	50	100
Grounding resistance R / Ω	1,467	1,572	1,617	1,631	1,643	1,648
Change compared to the previous calculation	0	0,105	0,045	0,014	0,012	0,005
Relative change compared to the previous calculation / %	0	7,16	2,86	0,87	0,74	0,31
Error in relation to the IEEE Std 80-2000 / %	−13,71	−7,53	−4,88	−4,06	−3,35	−3,06

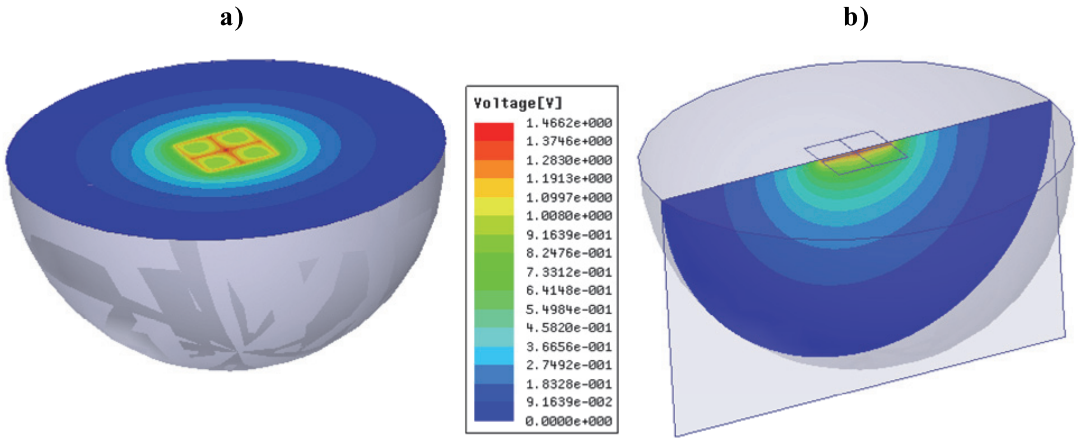

Figure 12 a) Scalar electric potential on the ground surface; b) Scalar electric potential along the cross section of the computational domain

6 RESULTS ANALYSIS

The behavioural trend of the scalar electric potential curves (Fig. 10) for different ratios R_b/L is consistent with the theoretical prediction. According to the previously presented theory, as the distance of the boundary conditions from the centre of the grounding conductor increases the potential curves become more stretched both vertically and horizontally. Vertical elongation is manifested in larger numerical amounts of the potential for a certain radial distance as ratio R_b/L increases. Horizontal elongation manifests itself in such a way that a larger radial distance is required for the potential to decrease to zero. More precisely, the potential drops to zero at the radial distance at which the boundary conditions are set to zero. Since the potential curves are very close to each other, the potential change is shown only up to a radial distance corresponding to twice the length of the grounding conductor. This achieved clarity of the graphical representation, but the information that the potential of all curves (except for curve $R_b/L = 2$) decreases to zero at the radial distance at which the boundary conditions are set to zero has disappeared.

Since the grounding resistance is a physical quantity calculated from the potential, it is to be expected that the distance of the boundary conditions from the centre of the grounding system will have an impact on the accuracy of determining the grounding resistance. Just as the accuracy of the potential calculation is improved by moving the boundary conditions away from the centre of the grounding system, so the accuracy of determining the grounding resistance is improved by moving the boundary conditions away. In order to gain a better insight into the FEM error for a certain R_b/L ratio, Tab. 2 also shows the FEM error in relation to the result obtained by the analytical Eq. (35). At this point, it should be emphasised that the recommended expressions for the grounding resistance of certain grounding geometries are not exact expressions and they have a small but still a finite error. Using Tab. 2, the small but still a finite error obtained by their application makes it impossible to draw a definite conclusion as to what exactly is the FEM error for a certain R_b/L ratio. Nevertheless, since the error of analytical Eq. (35) is very small, the comparison of the FEM results and the analytical expression makes sense. Also, for a certain R_b/L ratio, the errors in Tab. 2 are more favourable (i.e. they are smaller) compared to Tab. 1. This will be taken into account when providing guidelines in a way that we consider less favourable results to be relevant for providing guidelines. From the quasi-static field theory, it is known that, in the far field region, a field acts as if it was caused by a spherical field source or a point field source. Therefore, for distant points in space, far from the grounding system of the arbitrary shape, the current field and electric potential in the soil act as if they were caused by a spherical grounding conductor. Because the transition from the near field to the far field is gradual, and depends on the complexity of the grounding system, the guidelines for the initial design phase and analysis of the grounding system using FEM will be given separately from the guidelines for more accurate calculations using FEM. In the initial design phase and analysis of the grounding system, when a larger error is acceptable, the distance of the edge of the hemispherical soil model, from the centre of the grounding system, must be at least 10 times greater than the equivalent dimension of the grounding system. Since for ratio R_b/L = 10, the conditions valid for the far field zone have not yet occurred, the error listed in Tab. 1, for ratio, which is 10%, should be understood only as an indicative value of an actual error. For more accurate calculations using FEM, and in the case of complex grounding systems, for which there are no analytical expressions with acceptable accuracy to verify FEM results, we recommend monitoring the convergence of results for different ratios, as shown in Tab. 2. In such cases, when the exact solution is not known, for the acceptable ratio R_b/L, a criterion can be taken when the relative change, compared to the previous calculation, falls below the acceptable amount, for example 1%. In the example of a vertical buried cylinder shown in this article, according to this criterion, an acceptable R_b/L ratio would be $R_b/L > 20$.

According to Tab. 2, as the ratio R_b/L increases, the convergence rate decreases, and is below 1% for $R_b/L > 20$. For the ratio $R_b/L > 20$, the accuracy improvement is insignificant, but the duration of the calculation is drastically increased due to the drastically higher number of finite elements. For example, on a personal computer (PC), in the configuration: CPU 11th Gen Intel Core i7-11700F 2.50 GHz/4.9 GHz, with 32.0 GB, for the ratio R_b/L = 50, it took about 10 minutes to calculate the grounding resistance.

By comparing the data in Tab. 3 and Tab. 2, the expectation of the same trend and similar level of error in the case of a complex grounding system as well as a simple grounding system was confirmed. As in the case of a vertical cylindrical grounding system, the exact value of the grounding resistance for the four mesh grounding grid is not known. Although the error is small, IEEE Std 80-2000 [24] does not state the error present in Fig. 11b. Therefore, the calculated error values in Tab. 3 can only serve as indicative values of the actual error.

It should be emphasised that the paper analyses a very simple grounding system, and that the soil is modelled as a homogeneous medium. In the case of more complex grounding systems, such as mesh grounding systems, and by respecting that the soil is vertically multi-layered (inhomogeneous medium), the duration of the numerical calculation would be drastically extended. This is taken into account in this paper when giving guidelines (recommendations) on the required R_b/L ratio for the acceptable calculation accuracy.

7 OTHER APPLICATIONS

Although FEM is not suitable for the solution of electromagnetic problems with an infinite and a semi-infinite domain, such as the problem of determining the grounding resistance, especially not for complex grounding systems, the results from this study have other applications as well. Particularly interesting are the applications for which FEM is suitable, such as solving electromagnetic problems in a heterogeneous medium. For example, for the analysis and interpretation of the resistivity data [24-27]. Namely, when measuring the earth resistance, simple electrical systems, which consist of only a few vertically buried cylindrical electrodes, are used. One such electrode system, called the Wenner electrode arrangement, is shown in Fig. 13. From the collected measurement data, it is necessary to conclude what the structure and parameters of the soil are. If data are collected for the purpose of geological research, the soil can be very inhomogeneous. The guidance given in this article for such an application would be as follows. The maximum distance of the current electrodes in the process of measuring the apparent soil resistance should be considered an equivalent dimension of the system. For the initial modelling phase, we recommend that the computational domain is at least 10 times larger than the spacing of the current electrodes ($R_b \geq 10 \cdot D_{equivalent}$) (Fig. 13). After the initial phase, for more accurate calculations using FEM, we recommend monitoring the convergence of results for different R_b/L ratios in order to evaluate the acceptability of the results.

When the soil has poor electrical conductivity at the installation site of the grounding system, then soil with better electrical conductivity is artificially added at the installation site of the grounding system. Then the soil is locally inhomogeneous (Fig. 14). Since BEM, unlike FEM, has difficulty in treating electromagnetic tasks in an inhomogeneous medium, such an electromagnetic task becomes suitable for FEM. Fig. 14 shows two examples of grounding systems i.e. grounding rod and grounding grid, which are buried in locally heterogeneous soil. In both examples at the installation site of the grounding system the soil with lower resistivity was artificially placed. The natural resistivity of the soil is denoted by ρ_2, and the resistivity of artificially added soil is denoted by ρ_1. In such cases, we recommend that instead of the equivalent dimension of the grounding system, a larger equivalent dimension be taken, i.e. the equivalent dimension of the additional soil.

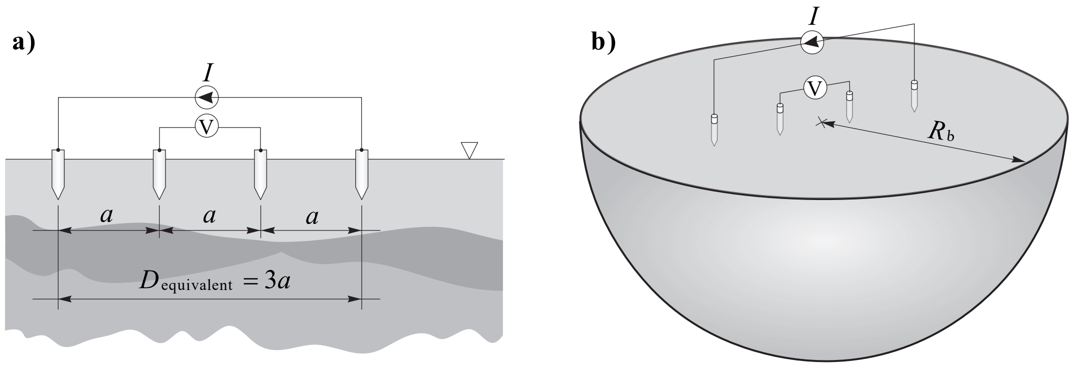

Figure 13 a) 2D graphic representation of the heterogeneous soil and the Wenner electrode arrangement; b) 3D graphic representation of the Wenner electrode arrangement and hemispherical soil model, i.e. computational domain. Computational domain size and size of measurement setup are not in scale

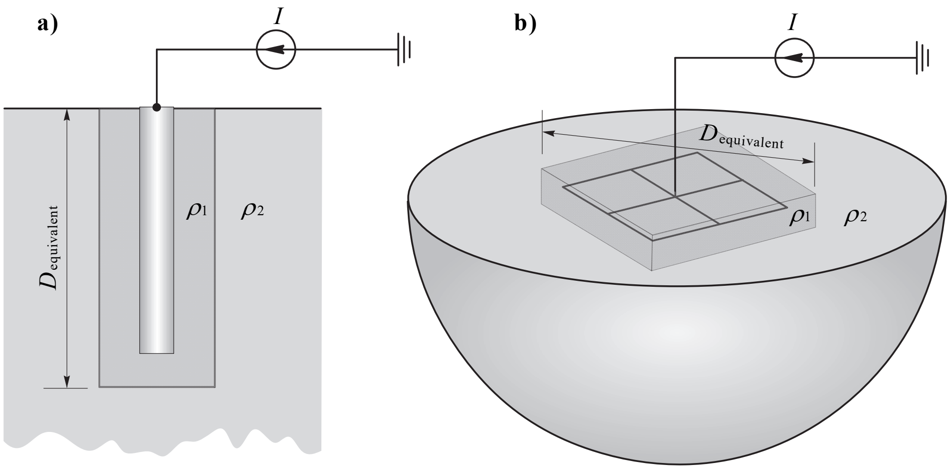

Figure 14 a) 2D graphic representation of the inhomogeneous ground (soil), vertical cylindrical conductor and current excitation; b) 3D graphic representation of the inhomogeneous ground (soil), grounding grid and current excitation

8 CONCLUSIONS

The paper presents the theoretical background in a simple and an unambiguous way, explaining the phenomenon of the influence of the computational domain size on the accuracy of determining the scalar electric potential and other physical quantities related to the scalar electric potential. As a compromise between the accuracy and duration of the calculation, when initially designing and analysing more complex grounding systems and heterogeneous soils, an error of about 10% seems acceptable, while for more demanding calculations, we recommend lower values, for example 5% or less. In the initial design phase and analysis of the grounding system, when a larger error is acceptable, the distance of the edge of the hemispherical soil model from the centre of the grounding system must be at least 10 times greater than the equivalent dimension of the grounding system. After the initial phase, for more accurate calculations using FEM, we recommend monitoring the convergence of results for different R_b/L ratios in order to evaluate the acceptability of the results. These guidelines are also applicable in other applications such as modelling as well as the analysis and interpretation of resistivity data using FEM.

9 REFERENCES

[1] Vijayaraghavan, G., Brown, M., & Barnes, M. (2004). *Practical Grounding, Bonding, Shielding and Surge Protection, Butterworth-Heinemann*. 1st edition, ISBN-13: 978-0-7506-6399-1.

[2] Bazelyan, E. M., & Raizer, Y. P. (2000). *Lightning Physics and Lightning Protection*. 1st edition, CRC Press, ISBN-10: 0-7503-0477-4.

[3] Majdandžić, F. (2004). *Uzemljivači i sustavi uzemljenja*. Graphis, Zagreb, ISBN-10: 953-96399-6-4.

[4] Ma, J. & Dawalibi, F. P. (2002). Analysis of grounding systems in soils with finite volumes of different resistivities. *IEEE Transactions on Power Delivery*, *17*(2), 596-602. https://doi.org/10.1109/61.997944

[5] Abdelkader, B., Boubakeur, Z., Tahar, S., & Yahia, S. (2020). Implentation and Design of Grounding Systems Using COMSOL multiphysics. *1st International Conference on Communications, Control Systems and Signal Processing (CCSSP)*, 513-517. https://doi.org/10.1109/CCSSP49278.2020.9151798

[6] Lorentzou, M. I., Kladas, A. G., & Hatziargyriou, N. D. (1999). Finite element modelling of grounding systems considering electrode geometry effects. *IEEE Transactions on Magnetics*, *35*(3), 1757-1760. https://doi.org/10.1109/20.767370

[7] Katsanou, V. N. & Papagiannis, G. K. (2009). Substation grounding system resistance calculations using a FEM approach. *IEEE Bucharest Power Tech*, 1-6. https://doi.org/10.1109/PTC.2009.5282044

[8] Hong T. P., Van, Q. D., & Viet, T. V. (2009). Grounding resistance calculation using FEM and reduced scale model. *IEEE Conference on Electrical Insulation and Dielectric Phenomena*, 278-281. https://doi.org/10.1109/CEIDP.2009.5377707

[9] Cavka, D., Poljak, D., & Goic, R. (2010). Transient analysis of ring shaped grounding electrode using isoparametric quadratic elements. *30th International Conference on Lightning Protection (ICLP)*, 1-5. https://doi.org/10.1109/ICLP.2010.7845768

[10] Trlep, M., Hamler, A., Jesenik, M., & Stumberger, B. (2003). The FEM-BEM analysis of complex grounding systems. *IEEE Transactions on Magnetics*, *3*(39), 1155-1158. https://doi.org/10.1109/TMAG.2003.810201
[11] Jinliang, H., Zeng, R., & Zhang, B. (2012). Numerical Analysis Method of Grounding. *IEEE Methodology and Technology for Power System Grounding*, 131-189. https://doi.org/10.1002/9781118255001.ch4
[12] Colominas, I., París, J., Guizán, R., Navarrina, F., & Casteleiro, M. (2015). Numerical Modelling of Grounding Systems for Aboveground and Underground Substations. *IEEE Transactions on Industry Applications*, *6*(51), 5107-5115. https://doi.org/10.1109/TIA.2015.2412521
[13] Liu, Z., Li, Z., & Wang, S. (2021). Test and Simulation of Transient Characteristics of a Grounding Grid in substation. *2021 International Conference on Advanced Electrical Equipment and Reliable Operation (AEERO)*, 1-4. https://doi.org/10.1109/AEERO52475.2021.9708335
[14] Sadiku, M. N. O. (2000). *Numerical Techniques in Electromagnetics*. 2nd edition, CRC Press, ISBN-10: 0-8493-1395-3.
[15] Haznadar, Z. & Štih, Ž. (2000). *Electromagnetic Fields, Waves, and Numerical Methods*. IOS Press, ISBN-13: 978-1586030643.
[16] Zienkiewicz, O. C., Taylor, R. L., & Zhu, J. Z. (2002). *The Finite Element Method: Its Basis and Fundamentals*. 6th edition, Elsevier, ISBN 978-0-7506-6320-5.
[17] Gibson, W. C. (2014). *The Method of Moments in Electromagnetic*. 2nd edition, Chapman and Hall/CRC, ISBN-13: 978-1-4822-3579-1.
[18] Uman, M. A. (2010). *The Art and Science of Lightning Protection*. 1st edition, Cambridge University Press, ISBN-13: 978-0-521-87811-1.
[19] Barić, T., Šljivac, D., & Stojkov, M. (2007). Validity Limits of the Expression for Measuring Soil Resistivity by the Wenner Method According to IEEE Standard 81-198. *Energija, Journal of Energy*, *56*(6), 730-753.
[20] IEEE Recommended Practice for Grounding of Industrial and Commercial Power Systems. *Institute of Electrical and Electronics Engineers*, (2007).
[21] *Grounding (earthing) and electromagnetic analysis software packages.* (2021, December 17). SES & technologies ltd.
[22] *Computer-aided engineering (CAE)/multiphysics engineering simulation software for product design and testing*. (2021, December 14). Ansys.
[23] *General-purpose simulation software based on advanced numerical methods.* (2021, December 17). Comsol.
[24] IEEE Guide for Safety in AC Substation Grounding, IEEE Std 80-2000 (Revision of IEEE Std 80-1986). *The Institute of Electrical and Electronics Engineers, Inc. New York*, (2000).
[25] IEEE Std 81-1983, IEEE Guide for Measuring Earth Resistivity, Ground Impedance and Earth Surface Potentials of a Ground System, (Revision of IEEE Std. 81 -1962). *The Institute of Electrical and Electronics Engineers, Inc., New York*, (1983).
[26] Lagace, P. J., Fortin, J., & Crainic, E. D. (1996). Interpretation of resistivity sounding measurements in N-layer soil using electrostatic images. *IEEE Transactions on Power Delivery*, *3*(11), 1349-1354. https://doi.org/.1109/61.517490
[27] Gaige Van Nostrand, R. & Cook, K. L. (1996). *Interpretation of Resistivity Data*. Geological Survey, US Department of the Interior, Washington, D. C. https://doi.org/10.3133/pp499

Contact information:

Tomislav BARIĆ, Full Professor, PhD
Faculty of Electrical Engineering,
Computer Science and Information Technology Osijek, University of Osijek,
Kneza Trpimira 2B, 31000 Osijek, Croatia
E-mail: tomislav.baric@ferit.hr

Hrvoje GLAVAŠ, Associate Professor, PhD
Faculty of Electrical Engineering,
Computer Science and Information Technology Osijek, University of Osijek,
Kneza Trpimira 2B, 31000 Osijek, Croatia
E-mail: hrvoje.glavas@ferit.hr

Željko HEDERIĆ, Full Professor, PhD
Faculty of Electrical Engineering,
Computer Science and Information Technology Osijek, University of Osijek,
Kneza Trpimira 2B, 31000 Osijek, Croatia
E-mail: zeljko.hederic@ferit.hr

Mirko KARAKAŠIĆ, Full Professor, PhD
(Corresponding author)
University of Slavonski Brod,
Mechanical Engineering Faculty in Slavonski Brod,
Trg Ivane Brlić Mažuranić 2, 35000 Slavonski Brod, Croatia
E-mail: mirko.karakasic@unisb.hr